Sensors and Actuators A 296 (2019) 316–323

Contents lists available at ScienceDirect

Sensors and Actuators A: Physical

journal homepage: www.elsevier.com/locate/sna

Electronically actuated microfluidic valves with zero static-power consumption using electropermanent magnets

Azam Gholizadeh [a], Siamak Abbaslou [b], Pengfei Xie [a], Ara Knaian [c], Mehdi Javanmard [a,*]

[a] Department of Electrical and Computer Engineering, Rutgers, The State University of New Jersey, Piscataway, NJ, USA
[b] Electrical Engineering Department, Princeton University, Princeton, NJ, USA
[c] NK Labs, LLC, Cambridge, MA, USA

ARTICLE INFO

Article history:
Received 30 January 2019
Received in revised form 27 May 2019
Accepted 17 June 2019
Available online 21 June 2019

Keywords:
Microfluidics valve
Electropermanent magnet
Zero static power
PDMS thin film

ABSTRACT

Valves are essential components for building integrated microfluidic circuits and enable control of fluidic transport for performing complex operations. Electronic actuation of microfluidic channels can enable fully integrated miniaturized fluidic systems with ultra-compact footprints. Here, we present a novel method for electronically actuating miniaturized microfluidic valves that consume zero-static power, using electropermanent magnets (EPM) in conjunction with elastomeric membranes. The proposed actuator design is compatible with standard soft-lithography fabricated channels allowing lab-on-a-chip researchers to integrate these valves in their existing Polydimethylsiloxane (PDMS) microfluidic systems. The use of electropermanent magnets enables zero static power consumption (holding mode), and uses on the order of millijoules of energy per actuation (switching/active mode). Using this configuration, we demonstrate on-demand control of fluidic transport in channels with a Y-junction. In this manuscript, we study and characterize the performance of EPM based valves using particle image velocimetry and compare the results with valves actuated using permanent magnets.

1. Introduction

Point-of-use biological, biomedical, and chemical analysis systems require the ability to transport and actuate fluids on the micro-scale while maintaining an ultra-compact instrumentation footprint. Over the last several decades, there has been an increasing interest in developing micro- Total Analysis Systems (MicroTAS) capable of performing controlled chemical and biochemical reactions on the micro-scale [1–5], which allows for minimizing chemical reagent consumption and improving assay speed due to enhanced transport and reaction kinetics [6–8]. In the context of biomedical applications [9–12], microfluidics have shown promise to enable portable point-of-care diagnostic assays [13]. Micro-valves for reliable control of micro-channels have enabled successful miniaturization and integration of lab on chip systems [14–17]. Despite immense progress made in miniaturization of fluid handling, the vast majority of solutions for controlling and actuating valves, to the best of our knowledge, requires costly bulky instrumentation [1,18,19]. Commercial instruments such as syringe pumps, peristaltic pumps, air-pressure sources, and solenoid valves are still the dominant tools used for precise sample injection and control in microfluidic systems [20–22]. The large size and complexity of these structures makes them incompatible with portable fully integrated devices.

For use in practical applications, valves need to be ultra-compact, low-cost, consume minimum power, and can be easily integrated into microfluidic devices. On-chip biological assays for analyzing proteins and DNA, such as immunoassays and Polymerase Chain Reaction (PCR), can involve multiple steps and a large number of valves, and thus low static power consumption is extremely important so EPM based micro-valves can be an important part of these devices [23–25]. Considering the wide use of soft-lithography for rapid prototyping of microfluidic devices, easing the integration of the valves/actuators into PDMS devices would enable users to efficiently adapt the technology into their own designs.

The most commonly used type of microfluidic valve is a membrane-based actuator. Microchannels, with a thin membrane acting as the actuator, are opened and closed by deformation of the membrane due to an external force. The force can be pneumatic [18,26], electrostatic [27,28], mechanical [29,30], thermal [31,32], or magnetic/electromagnetic [33–38], each with its own advantages and disadvantages. For example, a pneumatic valve normally requires a bulky external pressure source to operate, which makes miniaturization of the full platform challenging. Permanent-magnet valves involve moving parts. For example, an

* Corresponding author.
E-mail address: mehdi.javanmard@rutgers.edu (M. Javanmard).

https://doi.org/10.1016/j.sna.2019.06.037
0924-4247/© 2019 Published by Elsevier B.V.

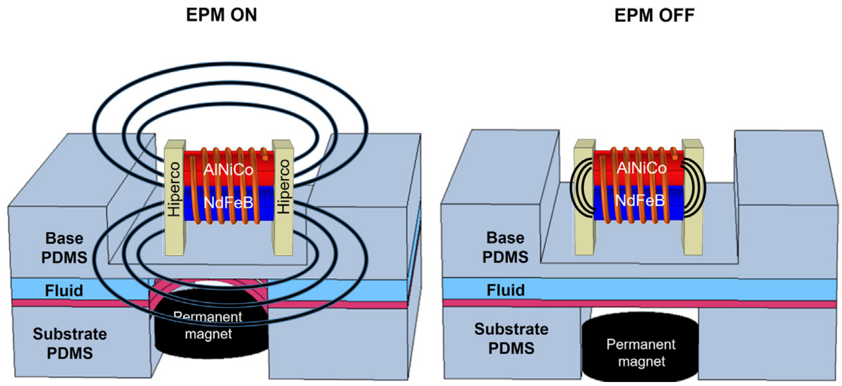

Fig. 1. Schematic of the concept of the electropermanent magnet (EPM) integrated with an elastomeric membrane. Applying a short current pulse switches ON or OFF the external magnetic field of the EPM, attracting or releasing the magnet below the elastomer membrane, thus closing and opening the valve respectively.

external motor is needed to displace the magnet. Localized actuation and lack of on-demand switching capability is difficult if the size of the magnet is large. Electrostatic and piezoelectric valves usually require continuous application of high voltage in order to generate sufficient force to actuate a membrane [37]. Electromagnetic valves involve no off-chip moving parts, use micro-fabricated coils and can be easily integrated with PDMS channels. However, they require large continuous currents to maintain the magnetic field to hold the valve in closed position, resulting in high static power consumption and significant joule heating.

Alternatively, electropermanent magnets (EPM), commonly used in large-scale industrial applications [39], provide the strong magnetic force offered by permanent magnets and the digital electronic control enabled by electromagnets without the requirement of large continuous current and the associated heating [40]. Additionally, EPMs provide localized actuation and require only a short current pulse to activate or deactivate the magnetic field. The zero static energy consumption of EPMs and the minimal dynamic energy consumption are ideal for applications requiring portability. Recently, miniaturized EPMs have found use in several novel applications including micromotors, programmable matter, and reconfigurable smartphones [41]. In recent work, wirelessly controlled low-power actuators using super-capacitor energy buffers in conjunction with EPMs have been demonstrated, showing their potential utility in portable systems [42]. In the context of lab on a chip research, an EPM actuator for droplet ferro-microfluidics was developed to sort droplets in a continuous flow microfluidic channel [43]. Electropermanent magnets have also been used in soft-robotics [47].

In this work, we present EPM actuated elastomeric membrane-based valves designed to control fluid flow in PDMS-based microfluidic systems. Fig. 1 shows the basic concept of the device. A microchannel was made with a thin deformable membrane at its base. A small magnet is placed below a thin PDMS membrane and an EPM is placed above the channel. Turning on the magnetic field will pull the small magnet towards the EPM, thus closing the channel, while turning the field off will release the magnet, thus opening the channel.

The EPM consists of a two permanent magnets that are bridged together by two millimeter sized magnetic rods, one hard (Neodymium-Iron-Boron) and one soft (Aluminum-Nickel-Cobalt). The hard magnet has higher magnetic coercivity (the resistivity of a magnetic material to changes in magnetization) compared to the soft magnet. An electromagnetic coil is wrapped around the two cylinders. In the default state, the EPM is ON because the hard and soft magnet have the same polarity. The magnetic field lines thus extend outside the EPM, around the full device, applying force to deform the membrane. When a short positive current pulse is applied across the EPM, the polarity of the soft magnet would be switched and turn into the opposite of that of the hard magnet, moving the magnetic field to a path entirely contained within the EPM, which allows the membrane to relax. In this state, the EPM is effectively OFF. To turn on the EPM, a negative current needs to be applied to bring back the polarity of the soft magnet to its initial condition.

In this EPM-based valve design, a short current pulse switches ON or OFF the magnetic field within microseconds and the deformation of membrane actuates the valve. First the EPMs were assembled and we characterized their magnetic behavior using various electrical excitation parameters. Second the capability of using the EPM for actuating microfluidic channels by fabricating and testing both simple rectangular and Y-junction channels was investigated. Then the mechanism of opening and closing of the valves was investigated in different flow conditions. In the next step, we compared the behavior of EPM-based valve with permanent magnet based valve in several different ranges of flow rates. To the best of our knowledge, this is the first use of EPMs to fabricate valves inside PDMS based microfluidic channels. These valves can serve as the building blocks in more complex designs with a network of channels serving as a microTAS system.

By applying a negative current pulse for a sufficiently long period of time, the magnetic field can be cancelled so the EPM-based valve is highly energy efficient. A key limitation of all magnetic valves is that the force from a magnetic dipole diminishes sharply with distance. Here, we use a thin substrate of PDMS with a thickness on the order of micrometers instead of glass, which enables us to minimize the distance between the EPM and the magnet below the deformable elastomeric membrane. The ability to rapidly switch on and off the EPM with controlled frequency in a repeatable manner can be used to implement pumping. A peristaltic pump can be built by fabricating three EPM valves serial to each other and applying a square wave pulse to each in peristaltic motion. Switchable permanent magnets involve moving parts and electromagnets require a continuous source of current. EPMs only require short pulses to be switched ON and OFF, and thus are attractive candidates for portable Micro Total Analysis Systems.

2. Materials and methods

2.1. Electropermanent magnet assembly

We fabricated and assembled the EPM based on the design previously developed by Knaian [40]. The schematic of the EPM set up is shown in Fig. 1. The ferromagnetic poles were cut from a 0.014″ thick Hiperco 50 coil (Ed Fagan Inc. Franklin Lakes, NJ). This Iron-Cobalt-Vanadium alloy has desirable magnetic properties such as

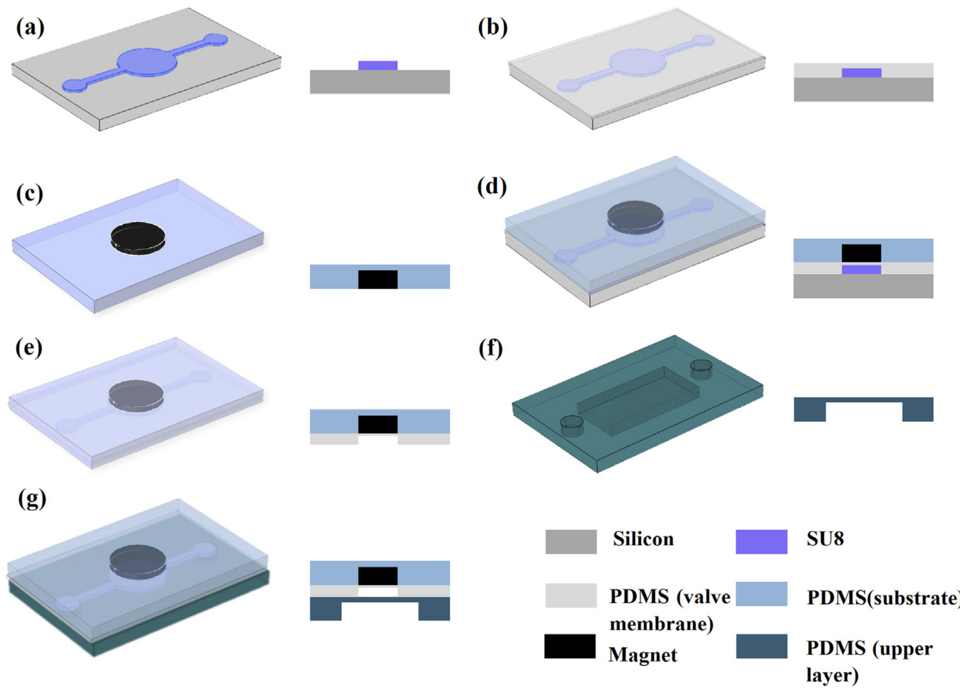

Fig. 2. Microfluidic valve fabrication steps. a) Soft lithographic patterning of SU-8 mold (flow channel pattern) on a silicon wafer, b) Spin coating of PDMS on the mold, c) Fabrication of PDMS substrate layer contains hole to embed tiny magnet, d) Bonding PDMS substrate layer onto the spin coated PDMS membrane using oxygen plasma bonding, e) Removing the two PDMS layers from the mold, f) Fabrication base PDMS layer to hold the EPM, g) Bonding of the all three layers together with oxygen plasma.

low coercivity and low A.C. core loss [44] that allows fast magnetic switching. High magnetic saturation of this material grants the poles to magnetize to the full amount of the magnetization without saturation. Two cylindrical magnets (2 mm diameter × 3 mm length) with same remnant magnetization but different coercivity were used. Sintered Neodymium Iron Boron Magnet (NdFeB model N38SH) and cast Aluminum Nickel Cobalt (Alnico grade LNG40) (BJA Magnetics, USA) were utilized as the hard and soft magnets respectively. The hard magnet has a coercivity (H_c) of 907 kA/m and a remnant magnetic flux (B_r) of 1.22 T and the soft magnet has a coercivity (H_c) 44 kA/m and a remnant magnetic flux (B_r) of 1.2 T. The pole pieces and the two magnets were assembled using Loctite Hysol E60-HP epoxy adhesive (Henkel, Westlake, OH). Mechanical pressure was applied overnight to fully bond the EPM pieces together. A length of 40 American wire gauge (AWG) insulated magnet wire (MWS Wire Industries) was used to make the coil.

2.2. Electropermanent magnet characterization

The EPM coil can be represented using an equivalent circuit consisting of an inductance in series with resistance. The resistance of the coil was measured with a digital multimeter that varies with the number of coil turns. The inductance of coil was measured by applying an AC sweep with a function generator and oscilloscope. To switch the EPM (from on to off or vice versa), a short pulse width with high current is required. The short pulse is provided with a programmable function generator which switches a MOSFET H-Bridge circuit to generate high power positive and negative pulses, commonly used to drive D.C. motors. The power was supplied from a D.C. power supply.

2.3. Fluidic device fabrication

Microfluidic chips were made of three layers of PDMS (Sylgard 184, Dow Corning) using standard soft lithography (Fig. 2). The SU-8 mold was patterned on a silicon wafer and then the microfluidic channel layer (10 ± 2 μm thickness) was cast onto the wafer by spin coating a 10:1 (v/v) ratio of base to curing agent with a spin rate of 4000 rpm and cured for 1 h at 80 °C. The thickness of this membrane is 15 ± 2 μm. A 2 mm top layer with an embedded tiny disc magnet (1.5 mm diameter) was attached to the channel membrane with oxygen plasma bonding. The whole structure was then peeled off from the silicon master mold wafer and bonded to the substrate layer. The thin part of the substrate polymeric layer is a 100 μm thick and 3 mm wide, designed to reduce the distance between the EPM and the valve.

3. Results and discussion

3.1. Electropermanent magnet operation

The EPM magnetic response was tested using an H-Bridge configuration circuit. A 120 μs positive current square pulse was applied to switch ON the EPM and the opposite current pulse was used to turn OFF the external magnetic field of EPM. The DC actuation voltage was applied and the current response was measured with a 0.1 Ω series resistor using an oscilloscope (Fig. 3a). The current response for a 120 turn coil EPM has a 7 μs time constant with a maximum current of 1.84 A. The maximum actuation time of the EPM, defined as $5\tau_{coil}$ [43], is 35 μs. Fig. 3b demonstrates the magnitude of the external magnetic field for different applied actuation voltages for the EPM (Fig. 3b inset) coil with 120 turns. The magnetic field was measured using the Hall-Effect probe of the gaussmeter. To study the magnetic behavior of EPM, the voltage was swept from 13 V to 30 V. A positive current pulse was used to turn ON the magnet. It shows as the blue curve in the figure. A negative current pulse was used to turn OFF the magnet (the red curve in the Fig. 3a). The results indicate that between 25 V to 30 V, the pulse has sufficient power to completely switch OFF the external magnetic field. As the voltage is increased, the amplitude of the magnetic field in the ON configuration raised. We have found that 13 V pulse does not carry sufficient power to perform magnetic switching. For the applied

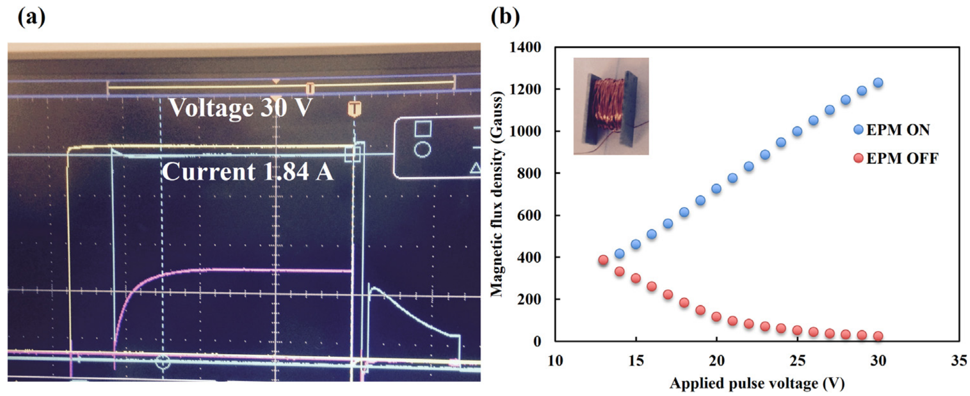

Fig. 3. a) Oscilloscope image of pulse properties required to switch EPM magnet. A 120 μs electrical pulse with activation voltage of 30 V is applied to switch an EPM with 120 Coil turns. b) The ON-OFF characterization of the EPM with respect to the applied pulse voltage. Inset shows the Image of a fabricated EPM (the distance between poles are 3 mm).

switching voltage of 30 V, the magnetic field strength (B field) for the EPM is estimated as 1.3 T and 0.02 T for the ON and OFF stages respectively. During the short (15 μs) switching of the EPM, it consumes 55.2 W of power (dynamic) and requires 6.6 mJ energy. The effect of the number of turns of the coil on the electromagnetic behavior of EPM was also investigated. Table 1 shows coil resistivity and maximum current pulse for different coil turns ranging from 80 to 150 and also the corresponding magnetic field intensity for the EPM in the ON and OFF states when applying 30 V.

3.2. Valve actuation simulation

Valve actuation was modeled using the finite element method in COMSOL multiphysics. The magnetic flux density was obtained for the ON and OFF states of the EPM. The remnant magnetic field of soft magnet was defined to be equal in magnitude, but opposite in direction of the hard magnet in the OFF state of EPM. For the ON state, the remnant magnetic field of the soft magnet was defined with the same magnitude in the same direction as the hard magnet. Fig. 4a shows the magnetic flux density of the EPM in the ON and OFF situation. In the OFF state, the external magnetic field is weak, on the other hand in the ON state there is strong external magnetic field, therefore there is maximal magnetic field in the valve area. To understand the time dependent valve deformation in response of the magnetic field, a 3D dimensional model of the channel was created. The magnetic field density was used to calculate the applied force on the valve membrane. Fig. 4b shows the simulation results of the valve membrane with 700 μm diameter and 10 μm thickness in the range of 100 μs. The channel thickness was designed as 30 μm thickness. In Fig. 4c, we can see the amount of displacement of the valve membrane with respect to time at 0.4 μs intervals. At the channel entrance, laminar flow with a speed of 100 μm/s was assumed and no slip condition was imposed on the channel walls. The membrane deformation was almost completed in 100 μs from the instant where magnetic force was applied.

Table 1
Electropermanent magnet properties.

EPM coil turns	EPM Properties (30 V Actuation)		
	Resistivity (Ohm)	Magnetic flux density when EPM is ON/OFF (Gauss)	Current (A)
80	6.4	1070/97	2.36
100	7.4	1070/76	2
120	8.2	1230/24	1.84
150	8.4	1240/18	1.76

3.3. EPM valve testing

To benchmark the performance of the microfluidic EPM valve, we built a Y-junction channel with two identical circular-shaped valves on two of the channels. Fluids of two different colors (green and red food dye) are injected into the two inlets (top of the device Fig. 5). When both valves are open, both fluids flow through the junction resulting in two laminar flow streams moving parallel to each other down a single channel until reaching the outlet. When one valve is closed and the other is open, only a single color of fluid will flow all the way to the outlet. Fig. 5 shows the steps of valve operation when switching the valve ON and OFF in the top right channel. When a negative current pulse was applied to the EPM, the magnetic force was cancelled and the valve remained open (Fig. 5c) and upon application of a positive current pulse, the thin membrane became deflected thus closing the valve (Fig. 5d). We experimentally determined that maximum performance is attained when the EPM is positioned vertically and the edge of the pole is located on top of the active valve area. The insets of Fig. 5 show the enlarged Y junction area for various valve states. The thickness of PDMS substrate is thinner on top of the valve compared to the other parts in order to minimize the distance between the EPM and the valve, thus maximizing magnetic field on top of the valve area. Capillary flow was the mechanism behind driving the fluid flow in this channel (no syringe pump).

We also studied the effect of pressure and the various modes of syringe pump operation on the valve response. The behavior of the valve immediately after applying a positive and negative pulse shown in Fig. 6. Fig. 6a shows the gradual injection of the green food dye into the junction as the valve in the top right channel is opened. Though the EPM response is on the order of tens of microseconds, the valve response time is on the order of several seconds. This delay in response time might be due to the diameter of the PDMS valve. Smaller circular valves can potentially improve the response time. In our current setup the channel width and height is 300 μm and 12 μm respectively, each valve is consists of a 700 μm diameter circle and the distance between the Y junction and the valve was 1 cm. A negative pulse was applied to actuate the EPM located on the upper right channel valve (red dye) that was initially in the closed state. Real time video demonstrating the opening of the valve can be found in the supplementary information. For the specific geometry fabricated, the response time for fully opening the valve and allowing fluid to flow through was approximately 6 s. Real-time closing of the valve is also demonstrated (Fig. 6b). In this case, the valve was initially open and a positive current pulse was applied which turns on the magnetic field of the EPM, thus closing the membrane stopping the red fluid from being injected

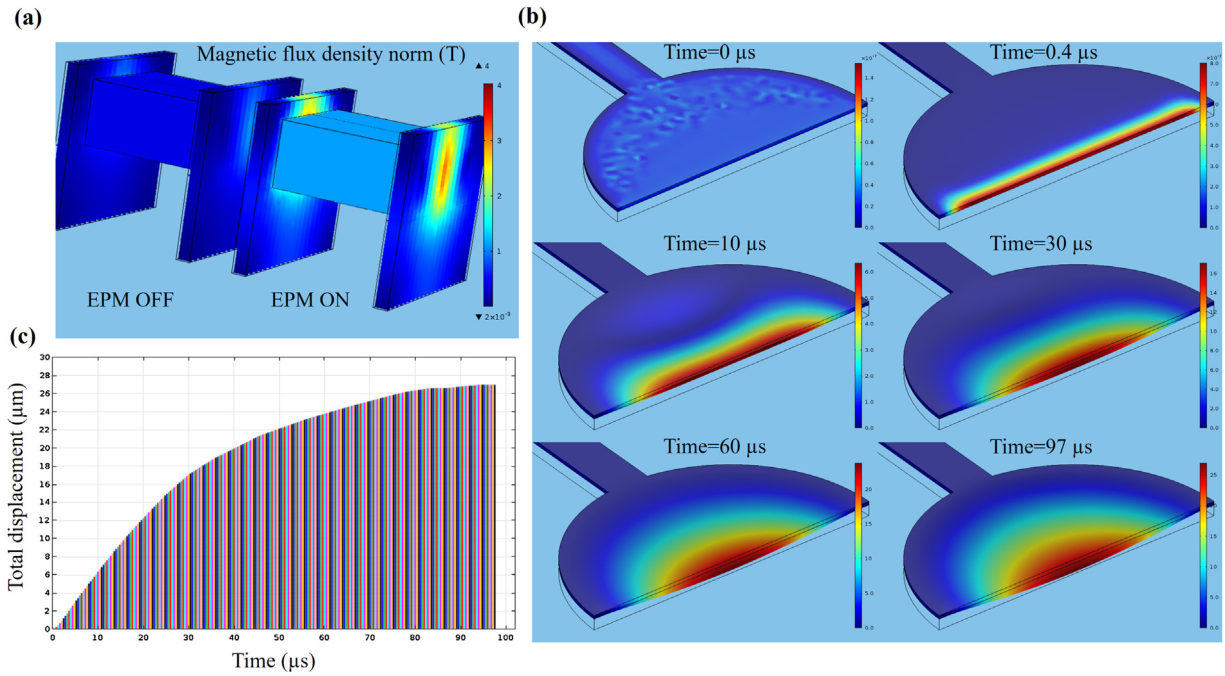

Fig. 4. Simulation of the EPM valve system. The EPM was simulated using the remnant magnetic field of the magnets. The microchannel was simulated at separation of 100 μm from the valve. a) Magnitude of magnetic flux density for EPM in OFF and ON states. b) Time dependent deformation of the thin membrane of the PDMS in the range of 100 μm on top of the 30 μm water channel. c) The plot of the membrane deformation versus the time for the valve with diameter of 700 um and initial water speed of 100 μm/s.

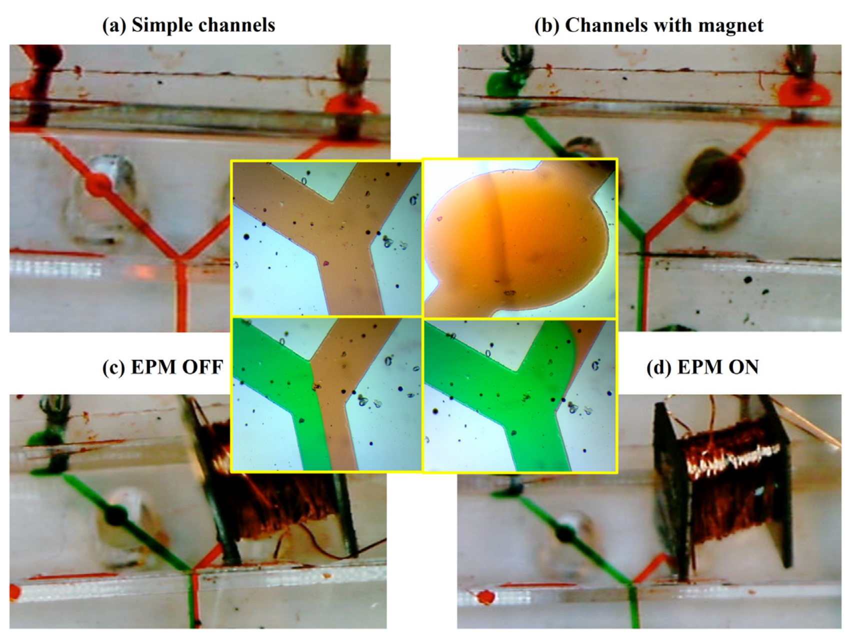

Fig. 5. a) Image of the 300 μm wide microfluidic channel with circular valves of 700 μm diameter, b) Channels are embedded with a 1.5 mm magnet, c) Y-junction state when EPM is OFF and top right inlet channel (injecting red fluid) is open, d) Y-junction state when EPM is ON and top right inlet channel (injecting red fluid) is closed. (For interpretation of the references to colour in this figure legend, the reader is referred to the web version of this article.)

in, allowing the green dye to fully be injected into the bottom channel towards the outlet. The response time for closing the valve in this configuration is approximately 6 s, however the time required to completely evacuate red dye from the main channel (lower left) was approximately 10 s. The real time video demonstrating closing of the valve can be found in supplementary information. This evaluation of the valve response time can be insightful for design of chemical reactions inside the channels, particularly when multiple reagents are involved.

3.4. Pressure characterization of EPM valve

We characterized the ability of the EPM valve to withstand fluid flow in channels of varying flow rates (for both fluid infusion and withdrawal). The performance of EPMs for actuating the valve was compared with that of permanent magnets. We used particle image velocimetry (3 μm beads) to precisely measure the drop in fluid speed inside the channel. To measure the fluid velocity, the suspension of beads was injected using a syringe pump, and the beads

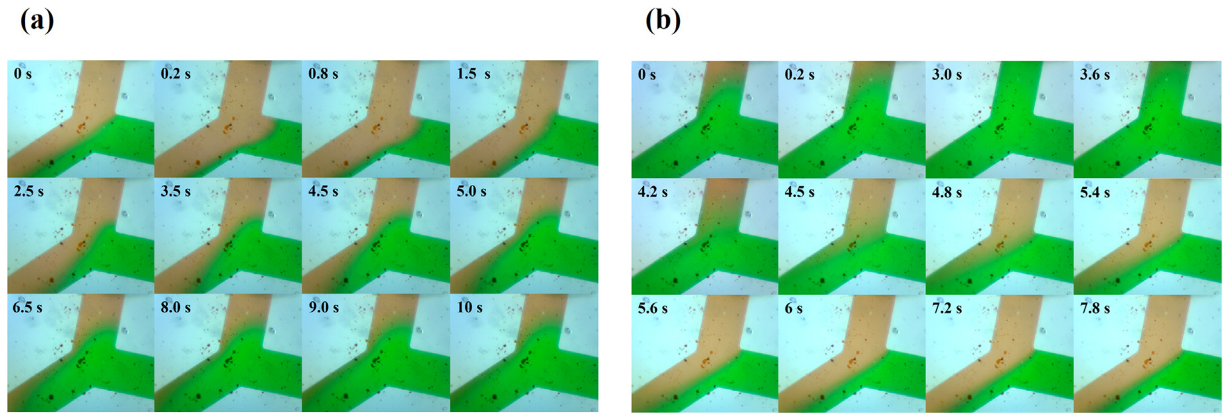

Fig. 6. a) Time lapse image of valve immediately after applying electrical pulse to EPM controlling top inlet channel allowing red food dye to get injected into junction. b) Time lapse image of valve immediately after applying electrical pulse to EPM closing the top inlet channel preventing red food dye from getting inject. Only the green food dye getting injected from the right inlet channel is fully passing through the junction into the outlet (left channel). (For interpretation of the references to colour in this figure legend, the reader is referred to the web version of this article.)

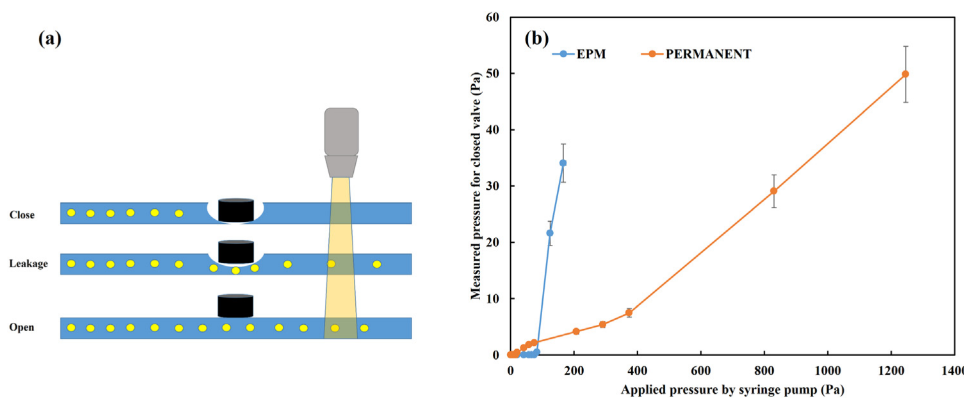

Fig. 7. a) A schematic of the experimental setup for optically estimating the pressure in the channel based on particle image velocimetry using 3 μm polystyrene beads. b) The y-axis shows the actual pressure measured in the channel when the magnetic valve is closed. The x-axis is the pressure that is being applied by the syringe pump. The performance of EPM and permanent magnet based valves are compared with each other in a simple rectangular channel structure. A syringe pump connected to the output withdraws fluid.

were tracked through optical microscope. This measurement was obtained for both the ON and OFF state of the EPM. (Fig. 7a). The recorded videos were converted to image frames, and the speed of the beads was calculated based on the average of five different measurements. Then the speed of the beads was converted to flow rate based on the cross sectional area of the channel and using the equation, $\Delta P = \frac{12\eta L}{Wh^3}Q$, it was converted to applied pressure. In this equation the parameters are as follows: L length, w width, h height of channel, Q on m^3/s and η viscosity of water. Fig. 7b shows the channel pressure measurements inside the channel for the withdrawal mode of the syringe pump in a range of 0.4–1250 Pa. In this experiment, a simple rectangular channel was used (instead of Y-shaped channels) to make sure the change in flow rate is due to the valves ability to fully withstand the applied pressure, rather than the fluid getting diverted to the adjacent channel. The measured pressure in the channel when the valve was closed was plotted against the pressure forced by the syringe pump. The results show that the EPM-driven valve can fully withstand and completely stop flow as long as the syringe pump is injecting fluid at less than 83 Pa pressure. When the syringe pump injects fluid at a pressure of 166 Pa, the valve remains 80% closed. The permanent magnet begins leaking at 20 Pa, but leaks at a slower rate compared to the EPM valve, and can remain 96% closed until 1250 Pa.

We also investigated the Y-shaped channels using food dye in the infusion mode of the syringe pump. Fig. 8 shows the results for applied pressure in the range of 1.2–42 kPa. The top right and the bottom right channels are the inlets. The left channel is the outlet. Fluid flows from right to left. The EPM valve is on in the top right channel. All images were taken after 10 s of applying a current pulse into the EPM. Based on these results, this valve can prevent fluid from passing until 25 kPa, and beyond that the valve no longer withstands the fluid pressure. Most of the fluid leakage stems from the edges of the valve. To minimize loss from the edges and withstand higher pressures, additional traps can be fabricated on the four sides of the circular part, thus increasing valve operation tolerance.

4. Conclusion

In this work, we designed, fabricated and tested a low power, electronically controlled, magnetically actuated elastomeric valve suitable for a wide range of microfluidic applications. Our fabrication process is simple and compatible with standard soft lithography processing and PDMS microfluidic channels, widely used in the lab on a chip community which allows microfluidic designers to easily integrate this technique in their chip fabrication workflow. Electropermanent magnets offer the electronic control of electromagnets, without the high static power consumption, while exhibiting the strong magnetic force of permanent magnets. As previously demonstrated, EPM control circuits with low power consumption can be realized using supercapacitors [42], thus making these novel valve structures suitable for integration

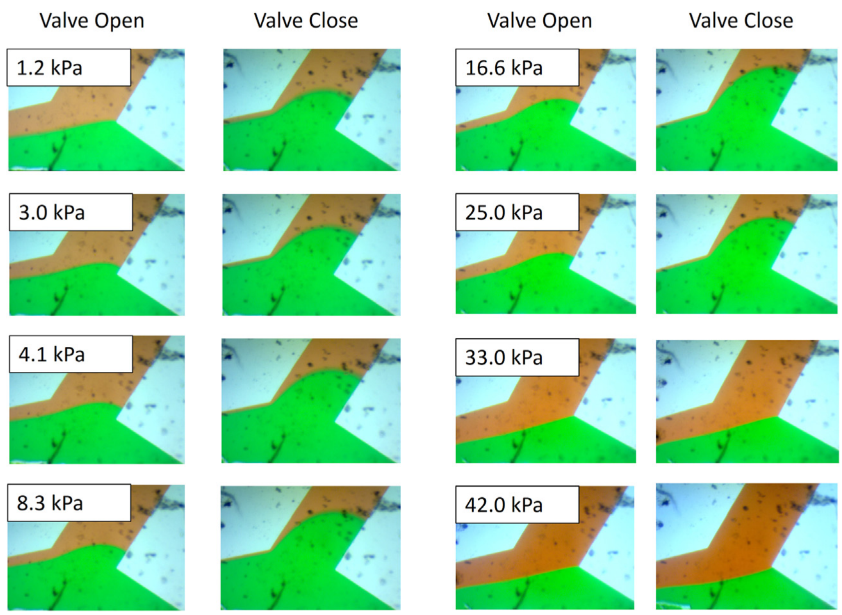

Fig. 8. Images at different applied pressures (1.2–42 kPa) of the Y-junction where the right channels is the inlet and the bottom left channel is outlet. The syringe pump is in infusion mode injecting red food dye in top right channel and green food dye in bottom right channel and directing both fluids through the Y-junction to the outlet (bottom left channel). EPM valve is controlling the top channel where red food dye is being injected. For each applied pressure, both the EPM ON and EPM OFF scenarios are visualized. (For interpretation of the references to colour in this figure legend, the reader is referred to the web version of this article.)

into point-of-care microfluidic devices. To design several valves in one device, the size of valve needs to be scaled. One solution to realize this involves using a control channel filled with magnetic particles instead of using hard magnets. In addition, EPMs can be isolated with PDMS walls to minimize interference between them. To enable practical integration into a large network of microfluidic channels, a 3D printed package can be developed for holding an array of electropermanent magnets, upon which the microfluidic channel substrate can be placed. Future efforts will be dedicated to build an array of EPMs, which enables on-chip peristaltic pumping and control of several channels for development of domain specific sample-to-answer systems. To enable large-scale fluidic integration, further miniaturization of the valves is feasible using micro-machining and microfabrication techniques [45,46]. Integration of magnetic actuators with microfluidic channels by incorporating microfabrication of the EPM can enable large scale integrated systems.

Acknowledgments

This work was performed at the electrical and computer engineering department and microelectronics research laboratory (MERL) at Rutgers University. This research was funded by the National Science Foundation (Grant numbers 1711165 and 1556253).

Appendix A. Supplementary data

Supplementary material related to this article can be found, in the online version, at doi:https://doi.org/10.1016/j.sna.2019.06.037.

References

[1] T. Thorsen, S.J. Maerkl, S.R. Quake, Microfluidic large-scale integration, Science 298 (2002) 580–584.
[2] S. Haeberle, R. Zengerle, Microfluidic platforms for lab-on-a-chip applications, Lab Chip 7 (2007) 1094–10110.
[3] L. Chen, A. Manz, P.J. Day, Total nucleic acid analysis integrated on microfluidic devices, Lab Chip 7 (2007) 1413–1423.
[4] K.i. Ohno, K. Tachikawa, A. Manz, Microfluidics: applications for analytical purposes in chemistry and biochemistry, Electrophoresis 29 (2008) 4443–4453.
[5] W. Li, Y. Zhang, C.P. Reynolds, D. Pappas, Microfluidic separation of lymphoblasts for the isolation of acute lymphoblastic leukemia using the human transferrin receptor as a capture target, Anal. Chem. 89 (2017) 7340–7347.
[6] S. Böhm, G. Burger, M. Korthorst, F. Roseboom, A micromachined silicon valve driven by a miniature bi-stable electro-magnetic actuator, Sens. Actuators A Phys. 80 (2000) 77–83.
[7] M.J. Madou, G.J. Kellogg, LabCD: a centrifuge-based microfluidic platform for diagnostics, systems and technologies for clinical diagnostics and drug discovery, Int. Soc. Opt. Photon. (1998) 80–94.
[8] G.M. Whitesides, The origins and the future of microfluidics, Nature 442 (2006) 368–373.
[9] M. Javanmard, S. Emaminejad, C. Gupta, J. Provine, R. Davis, R. Howe, Depletion of cells and abundant proteins from biological samples by enhanced dielectrophoresis, Sens. Actuators B Chem. 193 (2014) 918–924.
[10] Z. Lin, X. Cao, P. Xie, M. Liu, M. Javanmard, PicoMolar level detection of protein biomarkers based on electronic sizing of bead aggregates: theoretical and experimental considerations, Biomed. Microdevices 17 (2015) 1–7.
[11] J. Mok, M.N. Mindrinos, R.W. Davis, M. Javanmard, Digital microfluidic assay for protein detection, Proc. Natl. Acad. Sci. 111 (6) (2014) 2110–2115.
[12] P. Xie, X. Cao, Z. Lin, M. Javanmard, Top-down fabrication meets bottom-up synthesis for nanoelectronic barcoding of microparticles, Lab Chip 17 (2017) 1939–1947.
[13] E.K. Sackmann, A.L. Fulton, D.J. Beebe, The present and future role of microfluidics in biomedical research, Nature 507 (2014) 181–189.
[14] M.J. Madou, L.J. Lee, S. Daunert, S. Lai, C.-H. Shih, Design and fabrication of CD-like microfluidic platforms for diagnostics: microfluidic functions, Biomed. Microdevices 3 (2001) 245–254.
[15] D.J. Beebe, J.S. Moore, J.M. Bauer, Q. Yu, R.H. Liu, C. Devadoss, et al., Functional hydrogel structures for autonomous flow control inside microfluidic channels, Nature 404 (2000) 588–590.
[16] R. Greiner, M. Allerdissen, A. Voigt, A. Richter, Fluidic microchemomechanical integrated circuits processing chemical information, Lab Chip 12 (2012) 5034–5044.
[17] P. Frank, J. Schreiter, S. Haefner, G. Paschew, A. Voigt, A. Richter, Integrated microfluidic membrane transistor utilizing chemical information for on-chip flow control, PLoS One 11 (2016), e0161024.
[18] M.A. Unger, H.-P. Chou, T. Thorsen, A. Scherer, S.R. Quake, Monolithic microfabricated valves and pumps by multilayer soft lithography, Science 288 (2000) 113–116.
[19] G.A. Cooksey, C.G. Sip, A. Folch, A multi-purpose microfluidic perfusion system with combinatorial choice of inputs, mixtures, gradient patterns, and flow rates, Lab Chip 9 (2009) 417–426.
[20] R. Mayr, M. Haider, R. Thünauer, T. Haselgrübler, G.J. Schütz, A. Sonnleitner, et al., A microfluidic platform for transcription-and amplification-free detection of zepto-mole amounts of nucleic acid molecules, Biosens. Bioelectron. 78 (2016) 1–6.

[21] M. Ghodbane, E.C. Stucky, T.J. Maguire, R.S. Schloss, D.I. Shreiber, J.D. Zahn, et al., Development and validation of a microfluidic immunoassay capable of multiplexing parallel samples in microliter volumes, Lab Chip 15 (2015) 3211–3221.
[22] W. Jung, J. Han, J.-W. Choi, C.H. Ahn, Point-of-care testing (POCT) diagnostic systems using microfluidic lab-on-a-chip technologies, Microelectron. Eng. 132 (2015) 46–57.
[23] P. Neužil, S. Giselbrecht, K. Länge, T.J. Huang, A. Manz, Revisiting lab-on-a-chip technology for drug discovery, Nat. Rev. Drug Discov. 11 (2012) 620–632.
[24] E.A. Oblath, W.H. Henley, J.P. Alarie, J.M. Ramsey, A microfluidic chip integrating DNA extraction and real-time PCR for the detection of bacteria in saliva, Lab Chip 13 (2013) 1325–1332.
[25] M. Junkin, S. Tay, Microfluidic single-cell analysis for systems immunology, Lab Chip 14 (2014) 1246–1260.
[26] G. Thuillier, C.K. Malek, Development of a low cost hybrid Si/PDMS multi-layered pneumatic microvalve, Microsyst. Technol. 12 (2005) 180–185.
[27] D. Anjewierden, G.A. Liddiard, B.K. Gale, An electrostatic microvalve for pneumatic control of microfluidic systems, J. Micromech. Microeng. 22 (2012), 025019.
[28] K. Yoshida, S. Tanaka, Y. Hagihara, S. Tomonari, M. Esashi, Normally closed electrostatic microvalve with pressure balance mechanism for portable fuel cell application, Sens. Actuators A Phys. 157 (2010) 290–298.
[29] I. Fazal, M. Louwerse, H. Jansen, M. Elwenspoek, Stepper motor actuated microvalve, J. Phys. Conf. Ser. (2006) 1032, IOP Publishing.
[30] D.B. Weibel, M. Kruithof, S. Potenta, S.K. Sia, A. Lee, G.M. Whitesides, Torque-actuated valves for microfluidics, Anal. Chem. 77 (2005) 4726–4733.
[31] T. Lisec, S. Hoerschelmann, H. Quenzer, B. Wagner, W. Benecke, Thermally driven microvalve with buckling behaviour for pneumatic applications, micro electro mechanical systems, in: 1994, MEMS'94, Proceedings, IEEE Workshop on, IEEE, 1994, pp. 13–17.
[32] C. Megnin, M. Kohl, Shape memory alloy microvalves for a fluidic control system, J. Micromech. Microeng. 24 (2013), 025001.
[33] E.T. Carlen, C.H. Mastrangelo, Surface micromachined paraffin-actuated microvalve, J. Microelectromech. Syst. 11 (2002) 408–420.
[34] M. Pugliese, F. Ferrara, A.P. Bramanti, G. Gigli, V. Maiorano, In-plane cost-effective magnetically actuated valve for microfluidic applications, Smart Mater. Struct. 26 (2017), 045033.
[35] Z. Cai, J. Xiang, B. Zhang, W. Wang, A magnetically actuated valve for centrifugal microfluidic applications, Sens. Actuators B Chem. 206 (2015) 22–29.
[36] A. Gholizadeh, M. Javanmard, Magnetically actuated microfluidic transistors: miniaturized micro-valves using magnetorheological fluids integrated with elastomeric membranes, J. Microelectromech. Syst. 25 (2016) 922–928.
[37] W. Wang, Z. Yao, J.C. Chen, J. Fang, Composite elastic magnet films with hard magnetic feature, J. Micromech. Microeng. 14 (2004) 1321.
[38] A. Gholizadeh, M. Javanmard, Magnetically actuated microfluidic transistors: miniaturized micro-valves using magnetorheological fluids integrated with elastomeric membranes, J. Microelectromech. Syst. 25 (2016) 922–928.
[39] N.A. Shirazee, A. Basak, Electropermanent suspension system for acquiring large air-gaps to suspend loads, IEEE Trans. Magn. 31 (1995) 4193–4195.
[40] A.N. Knaian, Electropermanent Magnetic Connectors and Actuators: Devices and Their Application in Programmable Matter, Massachusetts Institute of Technology, 2010.
[41] A.N. Knaian, K.C. Cheung, M.B. Lobovsky, A.J. Oines, P. Schmidt-Neilsen, N.A. Gershenfeld, The milli-motein: a self-folding chain of programmable matter with a one centimeter module pitch, intelligent robots and systems (IROS), in: 2012 IEEE/RSJ International Conference on, IEEE, 2012, pp. 1447–1453.
[42] D.K. Abeywardana, A.P. Hu, Z. Salcic, Pulse controlled microfluidic actuators with ultra low energy consumption, Sens. Actuators A Phys. 263 (2017) 8–22.
[43] J.I. Padovani, S.S. Jeffrey, R.T. Howe, Electropermanent magnet actuation for droplet ferromicrofluidics, Technology 4 (2016) 110–119.
[44] T.V. Jayaraman, Effect of processing of HIPERCO® 50 alloy laminates on their magnetic properties, J. Electron. Mater. 44 (2015) 4379–4386.
[45] D.P. Arnold, N. Wang, Permanent magnets for MEMS, JMEMS 18 (2009) 1255–1266.
[46] M. Han, Q. Yuan, X. Sun, H. Zhang, Design and fabrication of integrated magnetic MEMS energy harvester for low frequency applications, JMEMS 23 (2014) 204–2012.
[47] A.D. Marchese, C.D. Onal, D. Rus, Soft robot actuators using energy-efficient valves controlled by electropermanent magnets, in: In 2011 IEEE/RSJ International Conference on Intelligent Robots and Systems 2011 Sep 25, IEEE, 2019, pp. 756–761.

Biographies

Azam Gholizadeh received the B.S. and M.S. degrees in chemistry, and the Ph.D. degree in nanotechnology from the Sharif University of Technology, Tehran, Iran, in 2005, 2007, and 2012 respectively. She received the Ph.D. degree in electrical engineering from Rutgers University at 2019. She currently is a postdoctoral associate in Electrical Engineering Department at Rutgers University. Her main research interests are micro/nanosystem technology, biosensors, microfluidics, and electrochemistry.

Siamak Abbaslou received a master's degree from TMU university, Iran with a focus on Nonlinear Optics and Solid State Electronics in 2012, and Ph.D. degree in Electrical Engineering from Rutgers University, New Jersey in 2017. Since 2017 he has been with the Lightwave Communications Group, Department of Electrical Engineering, Princeton University, Princeton, New Jersey, where he is engaged in development of integrated photonic devices including optical modulators, photonic systems for nonlinear signal processing and photonic neuromorhic computing applications. He is the recipient of the Award for Excellence in Solid State Electronics from the Rutgers Department of Electrical and Computer Engineering.

Pengfei Xie received his M.S degree in Electrical Engineering from Rutgers University in 2016. He is currently pursuing his PhD degree in the Department of Electrical Engineering at Rutgers. His research interests include impedance based protein assays, microfluidic medical devices, and point of care sensors.

Ara Knaian received the S.B and Ph.D. degrees from the Massachusetts Institute of Technology in 1999 and 2010, respectively. He is a principal engineer and managing partner at NK Labs in Cambridge, MA, USA. His research interests include applied electromagnetics, novel sensors and actuators, energy conversion, low-power circuit techniques, and robotics.

Mehdi Javanmard is an associate professor in the Electrical and Computer Engineering Department at Rutgers University. He received his BS (2002) from Georgia Institute of Technology and the MS in Electrical Engineering at Stanford University (2004). In 2008, he received his PhD in Electrical Engineering at Stanford University. Also at Stanford, he worked as a postdoctoral scholar from 2008 to 2009, and then as a staff engineering research associate from 2009 till 2014. In 2019 he was awarded the National Science Foundation CAREER Award. His interests lie in developing portable and wearable technologies for continuous health monitoring and understanding the effects of environment on health.